Turkish Journal of Computer and Mathematics Education *Vol.13 No.02 (2022), 451-474*

Research Article

Numerical Simulation of Oncolytic M1 Cancer Virotherapy Reaction-Diffusion Model by Collocation of B-Splines

Rohit Goel [a], Prof. R.C. Mittal[b], Dr. Neha Ahlawat[c]

[a] Research Scholar, Jaypee Institute of Information Technology, Noida & Assistant Professor, Deshbandhu College (University of Delhi)
[b]Professor, Department of Mathematics, Jaypee Institute of Information Technology
[c] Assistant Professor, Department of Mathematics, Jaypee Institute of Information Technology

Abstract: Cancer is a leading cause of death worldwide. Invention of better cancer treatment strategies remained a burning topic of the research since decades. Oncolytic virotherapy being a targeted type therapy is an emerging technology that uses selective engineered viruses to treat cancerous malignancies. The dynamics of oncolytic M1 virotherapy with spatial effects and anti-tumour immune responses cab better be studied and analysed with reaction-diffusion mathematical models. A reaction-diffusion mathematical model to characterize the dynamics of oncolytic M1 alphavirus in the cancer treatment virotherapy with immune responses is studied in this paper. A numerical simulation technique based on the collocation of cubic B-splines is proposed to approximate the solution of the considered reaction-diffusion model. Collocation forms of the partial differential equation results in a system of first order ordinary differential equations which in turn have been solved by Runge-Kutta method of order 4. The non-linearity of the model is being resolved without any transformation or linearization. The computed numerical results are in good agreement with those expected. Easy to apply and achieving accurate solutions in less CPU time are the key points of the present approach.

Keywords: Cancer, Oncolytic M1 virotherapy, Reaction-Diffusion model, Cubic B-splines, basis functions, Tri-diagonal matrix, Runge-Kutta (RK4) method.

1. Introduction

Cancer is potentially the collection of life-threatening diseases that occur due to the unconstrained growth of anomalous cells. Clusters of such abnormal cells form cancerous tumours. As per the estimation of International Agency for Research on Cancer (IARC) [1] on global cancer burden, it has risen to 19.3 million cases and 10 million cancer deaths in 2020. Due to COVID-19 pandemic, the diagnosis and the treatment of cancer is somehow obstructed [2] that may lead to a momentary drop in recent cancer cases but ultimately be followed by advanced stages to increased mortality. Depending upon the type and the stage of the cancer [3], there are many treatment strategies like surgery, radiation therapy, chemotherapy, immunotherapy, targeted therapy, immune therapy, stem cell transplant and the precision medicines. Wang et. al. [4] proposed nanomedicines-based gas therapeutic cancer treatment strategy. Oncolytic virotherapy which uses replication-competent viruses to kill cancer cells is one of the emerging treatment prominent modalities for cancer treatment [5-8]. In the recent past years, oncolytic virotherapy is wide field of research in medical [9] and mathematical [10-11] sciences. The ability of the oncolytic therapy that uses selective oncolytic viruses to completely remove the tumour cells depends upon the potency of the therapy. Satisfactory results have been achieved in clinical trials for the development of various oncolytic viruses. However, there are some challenges [7-9] that need to be investigated more precisely to enhance the efficacy of this type of treatment strategies. It is a relevant field of research to study the complexity of the impacts of tumour-specific immune responses on oncolytic virotherapy [15].

In order to provide better insights into the complicated dynamics of oncolytic virotherapy mathematical models [10-13] have been proposed. The models are similar to that of HBV and HIV viral infection models [16,21] and are aimed to analyse the cancer treatment strategies more effectively. The effect of virus burst size on viral therapy is studied by Wang et. al. [8]. Malinzi et. al. [11] proposed a model to analyse the efficacy of oncolytic virotherapy with chemotherapy and established that this combined treatment strategy can be a better option if the correct optimal dosage is used.

The diffusion [14,16,19] of oncolytic viruses within the tumour cells makes the models best suitable to be treated mathematically. Tao and Guo [14] have studied a nonlinear system of partial differential equations with a moving boundary to analyse the movements of viruses and immune cells. The diffusion of oncolytic viruses characterized by the spatial and temporal distributions over the tumour cells has been studied through various reaction-diffusion mathematical models. Wang et. al. [12] assumed the diffusion in a bounded domain and proposed a reaction-diffusion model to study the dynamics. To study the effects of oncolytic virotherapy on the concentration of tumour cells in the presence of CTL immune responses Malinzi et. al. [7] obtained travelling wave solutions a reaction-diffusion model.

To study the impacts of using oncolytic M1 virus on the growth of tumour and normal cells Wang et. at. [48] formulated the following basic ordinary differential equation model

$$\begin{aligned}
\frac{dH(t)}{dt} &= \kappa - d\,H - \beta_1 H\,N\, - \beta_2 H\,Y \\
\frac{N(t)}{dt} &= \alpha_1\beta_1 H\,N - (d+\eta_1)\,N \\
\frac{Y(t)}{dt} &= \alpha_2\beta_2 H\,Y - \beta_3 Y\,V - \beta_4 Y\,Z - (d+\eta_2)Y \\
\frac{dV(t)}{dt} &= \mu + \alpha_3\beta_3 Y\,V - (d+\eta_3)V
\end{aligned} \tag{1.1}$$

where $H(t), N(t), Y(t), V(t)$ denote the concentrations of nutrient, normal cells, tumor cells and free M1 virus respectively.

Elaiw et. at. [17] extended the model (1.1) considering the effects of CTL immune responses on the oncolytic virotherapy. It was also assumed that all the components in the considered model undergo diffusion so that the proposed model took the form of a reaction-diffusion model comprising of a system of partial differential equations. The non-negativity and the boundedness of the solution and the stability of the equilibrium points are analysed in the extended model.

The reaction-diffusion mathematical models take the form of the systems of semi-linear parabolic partial differential equations and correspond to a wide range of physical and dynamical phenomena occurring in day-to-day life. The solutions of reaction-diffusion equations account to a wide range of behaviours together with self-organized patterns formation including the formation of travelling waves. Reaction-diffusion models serve as a framework for understanding complex biological patterns. In the present paper, the solutions of the reaction-diffusion model for oncolytic M1 virotherapy cancer treatment proposed by Elaiw et. al. [17] has been found numerically using the cubic B-splines collocation method. The splines which are piecewise polynomial functions [44] constitute an elegant framework for dealing with the discretization and the interpolation problems. In this paper, cubic B-splines are collocated over the finite elements to approximate the spatial variables and its derivatives. A system of first order ordinary differential equations is obtained which in turn is solved by the well-known Runge-Kutta method of order 4. The B-splines are preferred over the other traditional schemes for their inheritance of continuity and the small local support over the given partition of the domain. In combination with collocation, this significantly reduces the efforts for solving differential equations. This method provides efficient explicit solutions with high accuracy and minimal computational efforts. Mittal and Jain [33] proposed a scheme based on collocation of cubic B-splines to solve the non-linear parabolic partial differential equations numerically. Mittal and Tripathi [34] have suggested a numerical method to approximate the solutions of coupled-Burger's equation using collocation of modified B-spline collocation scheme. Mittal et al. [35-39] have proposed the collocation of cubic B-splines to approximate solutions of various linear and non-linear partial differential equations. The authors also used the proposed scheme for a larger dimension malaria infection reaction-diffusion model [49] and achieved the accurate solutions. Therefore, cubic B-splines collocation method is applied to solve the reaction-diffusion oncolytic M1 virotherapy model in [17]. The computed numerical results are found in good agreement with those already in the literature. This scheme is found to be simple and easy to implement.

This paper is organized as follows: In section 2, the reaction-diffusion model for the oncolytic M1 virotherapy considered in this paper is described. In section 3, the procedure to implement the proposed method is given. In section 4-7, the method is applied to the given model and the corresponding explanation is given. In section 8, the numerical simulations are given and the results are summarized in Section 9. In section 10, Conclusions are discussed that briefly summarize the numerical outcomes.

2.The reaction-diffusion oncolytic M1 virotherapy model

Elaiw et. al. [17] extended the model motivated and studied by [48] describing the oncolytic M1 virotherapy for cancer patient's treatment upon considering the effects of cytotoxic T-lymphocytes (CTLs) immune responses to destroy the tumour cells. The diffusion behaviour of the various cell concentrations gives rise to a system of partial differential equations in the form of the well-known reaction-diffusion Mathematical model.

The model studied and analysed in the present paper is as given below:

$$\begin{aligned}
\frac{\partial H(x,t)}{\partial t} &= D_H\,\Delta H + \kappa - d\,H - \beta_1 H\,N\, - \beta_2 H\,Y \\
\frac{\partial N(x,t)}{\partial t} &= D_N\,\Delta N + \alpha_1\beta_1 H\,N - (d+\eta_1)\,N \\
\frac{\partial Y(x,t)}{\partial t} &= D_Y\,\Delta Y + \alpha_2\beta_2 H\,Y - \beta_3 Y\,V - \beta_4 Y\,Z - (d+\eta_2)Y \\
\frac{\partial V(x,t)}{\partial t} &= D_V\,\Delta V + \mu + \alpha_3\beta_3 Y\,V - (d+\eta_3)V \\
\frac{\partial Z(x,t)}{\partial t} &= D_Z\,\Delta Z + \alpha_4\beta_4 Y\,Z - (d+\eta_4)Z
\end{aligned} \tag{2.1}$$

for $t > 0,\ x \in \Omega$, where $H(x,t),\ N(x,t),\ Y(x,t),\ V(x,t)$ and $Z(x,t)$ respectively denote the concentrations of the nutrient, normal cells, tumour cells, free oncolytic M1 viruses and CTL cells at any position *x* and time instant *t*. $\partial\Omega$ is the smooth boundary of the bounded and the continuous domain Ω. $\beta_4 Y\,Z$ and $\alpha_4\beta_4 Y\,Z$ are the rates at which the CTLs attack and kill the tumour cells and stimulate respectively. $\Delta = \frac{\partial^2}{\partial x^2}$ is the Laplacian operator and D_Λ denotes the diffusion coefficient of the componentΛ. The parameter η_4 denotes the natural death rate constant of CTLs.

The model is associated with the biologically intact, continuous and the non-negative initial conditions

$$\begin{aligned}
H(x,0) &= \psi_1(x) \\
N(x,0) &= \psi_2(x) \\
Y(x,0) &= \psi_3(x) \\
V(x,0) &= \psi_4(x) \\
Z(x,0) &= \psi_5(x)
\end{aligned} \tag{2.2}$$

and the homogeneous Neumann boundary conditions representing a natural dispersal barrier.

$$\frac{\partial H}{\partial \vec{n}} = \frac{\partial N}{\partial \vec{n}} = \frac{\partial Y}{\partial \vec{n}} = \frac{\partial V}{\partial \vec{n}} = \frac{\partial Z}{\partial \vec{n}} = 0\,; \quad t > 0,\ \ x \in \partial\Omega \tag{2.3}$$

where $\frac{\partial}{\partial \vec{n}}$ is the outward normal derivative on the boundary $\partial\Omega$. These boundary conditions signify that the cells and the viruses cannot cross the boundary [12].

3. Mathematical Formulation

The solution domain $[a,b]$ is partitioned into a mesh of uniform step size length

$$h = x_{i+1} - x_i = \frac{(b-a)}{n}\,;\ \ i = 0, 1, 2 \ldots\ldots, n-1$$

by the knots x_i where $i = 0, 1, 2 \ldots\ldots, n$ such that

$$a = x_0 < x_1 \ldots\ldots\ldots\ldots < x_n = b$$

Our numerical treatment for oncolytic M1 virotherapy reaction-diffusion model using the collocation method with cubic B-splines is to find the approximate solutions $H^n(x,t),\ N^n(x,t),\ Y^n(x,t),\ V^n(x,t),\ Z^n(x,t)$ to the exact solutions $H(x,t),\ N(x,t),\ Y(x,t),\ V(x,t),\ Z(x,t)$ respectively, in the form given below

$$H^n(x,t) = \sum_{j=-1}^{n+1} \sigma_j{}^{(H)}(t)\, C_j(x), \qquad a \le x \le b,\ t > 0 \tag{3.1}$$

$$N^n(x,t) = \sum_{j=-1}^{n+1} \sigma_j{}^{(N)}(t)\, C_j(x), \qquad a \le x \le b,\ t > 0 \tag{3.2}$$

$$Y^n(x,t) = \sum_{j=-1}^{n+1} \sigma_j{}^{(Y)}(t)\, C_j(x), \qquad a \le x \le b,\ t > 0 \tag{3.3}$$

$$V^n(x,t) = \sum_{j=-1}^{n+1} \sigma_j{}^{(V)}(t)\, C_j(x), \qquad a \le x \le b,\ t > 0 \tag{3.4}$$

$$Z^n(x,t) = \sum_{j=-1}^{n+1} \sigma_j{}^{(Z)}(t)\, C_j(x), \qquad a \le x \le b,\ t > 0 \tag{3.5}$$

where $\sigma_j{}^{(i)}(t)$; $i = H, N, Y, V, Z$ are the time dependent quantities to be determined from the boundary conditions and the collocation of differential equations.

And, $C_j(x)$ are the cubic B-splines basis functions at the knots, defined by:

$$C_j(x) = \frac{1}{h^3}\begin{cases} (x - x_{j-2})^3 & x \in [x_{j-2}, x_{j-1}) \\ (x - x_{j-2})^3 - 4(x - x_{j-1})^3 & x \in [x_{j-1}, x_j) \\ (x_{j+2} - x)^3 - 4(x_{j+1} - x)^3 & x \in [x_j, x_{j+1}) \\ (x_{j+2} - x)^3 & x \in [x_{j+1}, x_{j+2}) \\ 0 & otherwise \end{cases} \tag{3.6}$$

where the functions $C_{-1}, C_0, C_1, \ldots\ldots\ldots\ldots C, C_N, C_{n+1}$ form a basis over the domain $a \le x \le b$.

The values of the functions $C_j(x)$ and their two successive derivatives $C'_j(x)$, $C''_j(x)$ over the prescribed set of knots are given in Table 1 below.

Table 1: Cubic B-splines functions and their derivatives at the knots

	x_{j-2}	x_{j-1}	x_j	x_{j+1}	x_{j+2}
$C_j(x)$	0	1	4	1	0
$C'_j(x)$	0	-3/h	0	3/h	0
$C''_j(x)$	0	$6/h^2$	$-12/h^2$	$6/h^2$	0
$C_j(x)$	0	1	4	1	0

At a particular knot x_j, there exist only three cubic B-splines, namely C_{j-1}, C_j, C_{j+1}. Each of the cubic B-splines functions covers four elements so that each element is covered by four cubic B-splines functions.

In the proposed scheme, the solution is approximated as a linear combination of the cubic B-splines basis functions over the concerned approximation space.

Using the B-spline functions (3.6) in the approximate solution function (3.1), the approximate values of $H^n(x,t)$ and its first two successive derivatives at any time t and at a particular knot x_j can be expressed in terms of time-dependent parameters $\sigma_j{}^{(H)}(t)$ as:

$$\left.\begin{aligned} H_j &= {\sigma_{j-1}}^{(H)} + 4{\sigma_j}^{(H)} + {\sigma_{j+1}}^{(H)} \\ h{H'}_j &= 3({\sigma_{j+1}}^{(H)} - {\sigma_{j-1}}^{(H)}) \\ h^2{H''}_j &= 6({\sigma_{j+1}}^{(H)} - 2{\sigma_j}^{(H)} + {\sigma_{j+1}}^{(H)}) \end{aligned}\right\} \quad (3.7)$$

The corresponding values of the approximate solutions for the remaining four variables and their derivatives can be obtained in the similar manner.

4.Treatment at Boundary Conditions

If $k_0(t)$ and $k_1(t)$ are the Neumann boundary values of H respectively

$$\left(\frac{\partial H}{\partial x}\right)_{x=a} = k_0(t) \;\; and \;\; \left(\frac{\partial H}{\partial x}\right)_{x=b} = k_1(t) \quad (4.1)$$

Then the approximate solution of H can be written as

$$H_x(x_0,t) = \sum_{j=-1}^{1} {\sigma_j}^{(H)} {C'}_j(x_0) = k_0(t)$$
$$H_x(x_N,t) = \sum_{j=n-1}^{n+1} {\sigma_j}^{(H)} {C'}_j(x_n) = k_1(t) \quad (4.2)$$

Using the Table 1, we get,

$$\begin{aligned} {\sigma_1}^{(H)} - {\sigma_{-1}}^{(H)} &= \left(\frac{h}{3}\right) k_0(t) \\ {\sigma_{n+1}}^{(H)} - {\sigma_{n-1}}^{(H)} &= \left(\frac{h}{3}\right) k_1(t) \end{aligned} \quad (4.3)$$

so that

$$\begin{aligned} {\sigma_{-1}}^{(H)} &= {\sigma_1}^{(H)} - \left(\frac{h}{3}\right) k_0(t) \\ {\sigma_{n+1}}^{(H)} &= {\sigma_{n-1}}^{(H)} + \left(\frac{h}{3}\right) k_1(t) \end{aligned} \quad (4.4)$$

Thus, the two-time dependent quantities falling outside the prescribed knots are determined. The remaining other variables can also be treated at the boundary conditions similarly.

5. Implementation to a Reaction-Diffusion equation

The reaction-diffusion differential equation for $H(x,t)$ is given by:

$$\frac{\partial H(x,t)}{\partial t} = D_H \, \Delta H + \phi_1(H,N,Y,V,Z) \quad (5.1)$$

whereD_H is diffusion coefficient and the first term on the right-hand side of (5.1) represents the diffusion term and ϕ_1 represents the reaction term.

Using (3.7) in the approximate solution expression (3.1) for$H^n(x,t)$, the given differential equation (5.1) reduces to the following system of differential equations:

$$\dot{\sigma}_{j-1}{}^{(H)} + 4\dot{\sigma}_j{}^{(H)} + \dot{\sigma}_{j+1}{}^{(H)} = ({\sigma_{j-1}}^{(H)} - 2{\sigma_j}^{(H)} + {\sigma_{j+1}}^{(H)})D_H \; + \; \phi_{1j} \, 0 \le j \le n \quad (5.2)$$

ϕ_{1j} being the right-hand side of H at the j-th node. Upon eliminating $\dot{\sigma}_{-1}{}^{(H)}, \dot{\sigma}_{n+1}{}^{(H)}, {\sigma_{-1}}^{(H)}, {\sigma_{n+1}}^{(H)}$ using (4.4), the following system of differential equations is obtained:

$$A \, \dot{\hat{\boldsymbol{\sigma}}}^{(\boldsymbol{H})} = B_H \hat{\boldsymbol{\sigma}}^{(\boldsymbol{H})} \; + \; \widehat{\phi_1} \quad (5.3)$$

where

$$A = \begin{bmatrix} 4 & 2 & & & & & \\ 1 & 4 & 1 & & & & \\ & & \dots\dots\dots & & & & \\ & & \dots\dots\dots & & & & \\ & & & & 1 & 4 & 1 \\ & & & & & 2 & 4 \end{bmatrix}_{(n+1)\times(n+1)} \quad (5.4)$$

and

$$B_H = D_H . B \quad (5.5)$$

$$B = \left(\frac{6}{h^2}\right)\begin{bmatrix} -2 & 2 & & & & & \\ 1 & -2 & 1 & & & & \\ & & \dots\dots\dots & & & & \\ & & \dots\dots\dots & & & & \\ & & & & 1 & -2 & 1 \\ & & & & & 2 & -2 \end{bmatrix}_{(n+1)\times(n+1)} \quad (5.6)$$

and

$$\dot{\hat{\boldsymbol{\sigma}}}^{(\boldsymbol{H})} = \begin{bmatrix} \dot{\sigma}_0{}^{(H)} \\ \dot{\sigma}_1{}^{(H)} \\ \dots \\ \dots \\ \dots \\ \dot{\sigma}_{n-1}{}^{(H)} \\ \dot{\sigma}_n{}^{(H)} \end{bmatrix}, \widehat{\phi_1} = \begin{bmatrix} \phi_{10} + \left(\frac{h}{3}\right)k_0(t) \\ \phi_{11} \\ \dots \\ \dots \\ \dots \\ \phi_{1(n-1)} \\ \phi_{1n} - \left(\frac{h}{3}\right)k_1(t) \end{bmatrix}_{(n+1)\times 1} \quad (5.7)$$

Here, A is a tri-diagonal matrix of order $(n+1)$ and $\widehat{\phi_1}$ is the right-hand side column vector of order $(n+1)$.

Similar systems of differential equations can be described in the corresponding time dependent quantities for the remaining variables with their respective right hand side vectors.

6.Evaluation of the initial vector $\widehat{\boldsymbol{\sigma}^{\mathbf{0}}}^{(\boldsymbol{H})}$

The initial vector $\widehat{\boldsymbol{\sigma}^{\mathbf{0}}}^{(\boldsymbol{H})}$ can be obtained by using the given initial conditions and the boundary values of their derivatives.

$$H_x(a,0) = H_x(x_0,0) = k_0(0) \quad (6.1)$$

$$H(x_j,0) = \psi_1(x_j), \qquad j = 1,2 \dots\dots, n-1 \qquad (6.2)$$

$$H_x(b,0) = H_x(x_N,0) = k_1(0) \qquad (6.3)$$

Similar expressions will be obtained for the other remaining variables. Equations (6.1) - (6.3) on applying to (3.1) yields a $(n+1)\times(n+1)$ system of differential equations of the form

$$A\,\widehat{\sigma^0}^{(H)} = \widehat{\phi_1^0} \qquad (6.4)$$

where

$$\widehat{\sigma^0}^{(H)} = \begin{bmatrix} \sigma_{H0}^0 \\ \sigma_{H1}^0 \\ \dots \\ \dots \\ \dots \\ \sigma_{H(n-1)}^0 \\ \sigma_{Hn}^0 \end{bmatrix}, \qquad \widehat{\phi_1^0} = \begin{bmatrix} \psi_1(x_0) + \left(\frac{h}{3}\right)k_0(0) \\ \psi_1(x_1) \\ \dots \\ \dots \\ \dots \\ \psi_1(x_{n-1}) \\ \psi_1(x_n) - \left(\frac{h}{3}\right)k_1(0) \end{bmatrix}$$

and so on. This system being a tri-diagonal system can thus be solved by Thomas algorithm [42, 43] to get the initial coefficients of the B-splines functions in the approximated solution.

7. Implementation of the method

The considered oncolytic M1 virotherapy model for cancer treatment can be expressed in the standard reaction-diffusion form as:

$$\frac{\partial H(x,t)}{\partial t} = D_H\,\Delta H + \phi_1(H,N,Y,V,Z)$$
$$\frac{\partial N(x,t)}{\partial t} = D_N\,\Delta N + \phi_2(H,N,Y,V,Z)$$
$$\frac{\partial Y(x,t)}{\partial t} = D_Y\,\Delta Y + \phi_3(H,N,Y,V,Z)$$
$$\frac{\partial V(x,t)}{\partial t} = D_V\,\Delta N + \phi_4(H,N,Y,V,Z)$$
$$\frac{\partial Z(x,t)}{\partial t} = D_Z\,\Delta N + \phi_5(H,N,Y,V,Z)$$

where each of the $D_i^{'}s$ are the respective diffusion coefficients and the corresponding terms are the diffusion terms and ϕ_i represents the reaction terms in each the corresponding reaction-diffusion differential equations.

As stated above, using the B-splines approximation for the reaction diffusion system (7.1) – (7.5), we get the following system of ordinary differential equations

$$\boldsymbol{M}\,\dot{\hat{\boldsymbol{\sigma}}} = \boldsymbol{P}\,\hat{\boldsymbol{\sigma}} + \boldsymbol{F}$$

where M and P are the block diagonal matrices each of order $5(n+1)$.

$$\boldsymbol{M} = \begin{bmatrix} A & & & & \\ & A & & & \\ & & A & & \\ & & & A & \\ & & & & A \end{bmatrix}_{5(n+1)\times 5(n+1)}$$

and

$$\boldsymbol{P} = \begin{bmatrix} B_H \\ B_N \\ B_Y \\ B_V \\ B_Z \end{bmatrix}_{5(n+1)\times 5(n+1)}$$

Here $\dot{\hat{\boldsymbol{\sigma}}}$ and **F** are the column vectors of time dependent numbers and the right-hand side quantities respectively.

$$\dot{\hat{\boldsymbol{\sigma}}} = \begin{bmatrix} \dot{\hat{\sigma}}^{(H)} \\ \dot{\hat{\sigma}}^{(N)} \\ \dot{\hat{\sigma}}^{(Y)} \\ \dot{\hat{\sigma}}^{(V)} \\ \dot{\hat{\sigma}}^{(Z)} \end{bmatrix}, \qquad \mathbf{F} = \begin{bmatrix} \widehat{\phi_1} \\ \widehat{\phi_2} \\ \widehat{\phi_3} \\ \widehat{\phi_4} \\ \widehat{\phi_5} \end{bmatrix}_{5(n+1)\times 1}$$

The parameter vector $\dot{\hat{\boldsymbol{\sigma}}}$ in the above system of ordinary differential equations is determined at a specified time level using the Thomas algorithm. Then the approximate solutions at any desired time can be found by computing the time dependent coefficients in the approximated solution by using the RK4 method.

8. Numerical Simulations

Numerical simulations are performed to validate and implement the proposed scheme. For this purpose, the spatial domain $\varphi = [0,2]$ is considered with step size of $\Delta x = 0.1$. For calculations, the time step size of $\Delta t = 0.001$ is selected. The following parameter values as considered by [11,14] are taken: $\kappa = 0.02,\ \mu = 0.01,\ d = 0.02,\ \alpha_1 = 0.8,\ \alpha_3 = 0.5,\ \alpha_4 = 0.8,\ D_H = D_N = D_Y = 0.01,\ D_V = D_Z = 0.03.$ All the remaining parameters are taken as free parameters depending upon the corresponding cases classified by the stability analysis.

Depending upon the convergence of the positive solutions of the model and the global stability of the equilibrium points, the numerical simulations are performed under six different cases given below in Table 2. The detailed biological significances and the impacts of these six different cases are discussed in detail in the later section 9 of Results and Discussions.

Table 2: Parameters in different Cases

Cases	I	II	III	IV	V	VI
$\boldsymbol{\beta_1}$	0.03	0.03	0.1	0.04	0.15	0.15
$\boldsymbol{\beta_2}$	0.03	0.1	0.03	0.5	0.35	0.5
$\boldsymbol{\beta_3}$	0.1	0.1	0.1	0.1	0.1	0.05
$\boldsymbol{\beta_4}$	0.03	0.2	0.03	0.6	0.1	0.6
$\boldsymbol{\eta_1}$	0.04	0.04	0.008	0.05	0.008	0.008
$\boldsymbol{\eta_2}$	0.01	0.008	0.01	0.008	0.008	0.008
$\boldsymbol{\eta_3}$	0.008	0.008	0.006	0.005	0.008	0.005
$\boldsymbol{\eta_4}$	0.01	0.01	0.01	0.02	0.01	0.02
$\boldsymbol{\alpha_2}$	0.8	0.8	0.8	0.9	0.9	0.9

Depending upon the global stability of the equilibrium points for the competition-free equilibrium, the treatment failure immune-free equilibrium, the tumour-free equilibrium, the treatment failure equilibrium, partial success immune-free equilibrium and the coexistence equilibrium as discussed in [17] there are defined threshold positive numbers $R_0, R_1, R_2, \widetilde{R_p}, \widetilde{R_q}$ and $\widetilde{R_r}$ as:

$$R_0 = \frac{\kappa\alpha_2\beta_2}{d(d+\eta_2)}$$

$$R_1 = \frac{\kappa\alpha_1\beta_1}{d(d+\eta_1)}$$

$$R_2 = \frac{\alpha_4\beta_4(d+\eta_3)}{\alpha_3\beta_3(d+\eta_4)}$$

$$\widetilde{R_p} = \frac{\mu\beta_3}{(d+\eta_2)(d+\eta_3)}$$

$$\widetilde{R_q} = 1 + \frac{\beta_2(d+\eta_4)}{\alpha_4\beta_4 d}$$

$$\widetilde{R_r} = 1 + \frac{\beta_2(d+\eta_3)}{\alpha_3\beta_3 d}$$

This paper mainly concerns with the numerical simulation techniques to solve the oncolytic M1 virotherapy model for the cancer treatment. A detailed analysis of these threshold parameters and their biological aspects can be well studied in [17] and the available literature.

Two different sets of the initial values are taken under consideration for a better understanding and comparison of results. The first set of initial conditions for the model will be considered as similar to [40-41]

$$\begin{aligned}
\psi_1(x) &= 0.3\left(1 + 0.2\,cos^2(\pi x)\right)\\
\psi_2(x) &= 0.2\left(1 + 0.2\,cos^2(\pi x)\right)\\
\psi_3(x) &= 0.1\left(1 + 0.2\,cos^2(\pi x)\right)\\
\psi_4(x) &= 0.1\left(1 + 0.2\,cos^2(\pi x)\right)\\
\psi_5(x) &= 0.01\left(1 + 0.2\,cos^2(\pi x)\right)
\end{aligned} \tag{8.1}$$

Taking into account the biological aspects of the model, the following set of initial conditions are also considered:

$$\begin{aligned}
\psi_1(x) &= 0.3\,(1 + 0.2\,|\sin(\pi x)|)\\
\psi_2(x) &= 0.2\,(1 + 0.2\,|\sin(\pi x)|)\\
\psi_3(x) &= 0.1\,(1 + 0.2\,|\sin(\pi x)|)\\
\psi_4(x) &= 0.1\,(1 + 0.2\,|\sin(\pi x)|)\\
\psi_5(x) &= 0.01\,(1 + 0.2\,|\sin(\pi x)|)
\end{aligned} \tag{8.2}$$

9. Results and Discussions

In this section, the numerical solutions obtained by the proposed scheme for the given cancer oncolytic M1 virotherapy treatment reaction- diffusion model [17] are summarized by performing simulations for the six globally stability dependent different cases.

In Case I, for $R_0 < \widetilde{R_p}$ and $R_1 < 1$ the solutions lead to the competition free equilibrium asymptotically stable state. The simulated results are depicted in the Figures 1.1 and 1.2 for the two sets of the considered initial conditions. The cancer treatment strategy successfully eradicated the tumour cells but failed to restore the normal cells in the absence of immune responses, leading to the patient death.

In Case II, for $R_0 > \widetilde{R_p}$ and $R_2 > 1$, the oncolytic M1 virotherapy leads to the extinction of the normal cells and failed to remove the tumour cells in the absence of the immune responses. The simulated results are depicted in the Figures 2.1 and 2.2. The situation refers to the threatening case for the cancer patient's health.

In Case III, for $R_1 > 1$ and $R_0 < R_1 + \frac{\kappa\mu\alpha_1\beta_1\beta_3}{d(d+\eta_1)(d+\eta_2)(d+\eta_3)}$, in the absence of immune responses, the treatment strategy successfully removed the tumour cells with restoration of the normal cells that leads improvement of the patient's health. The simulated results are shown in the Figures 3.1 and 3.2.

In Case IV, for $R_2 > 1$, $R_0 > \widetilde{R_q} + \frac{\mu\gamma_2}{\alpha_3 d(d+\eta_2)(d+\eta_4)(R_2-1)}$ and $R_1 < \widetilde{R_q}$, in the presence of anti-tumor immune responses, leads to the remarkable decrease in the tumor-cells concentration which further degrades the concentrations of the oncolytic M1 virus concentration. This leads to the complete failure of the cancer treatment strategy. The results are summarized in the Figures 4.1 and 4.2.

In Case V, for $R_2 > 1$, $R_0 > R_1 + \frac{\kappa\mu\alpha_1\beta_1\beta_3}{d(d+\eta_1)(d+\eta_2)(d+\eta_3)}$, $\frac{R_0}{R_1} > 1, \widetilde{R_r} < R_1 + \frac{\mu\beta_2}{\alpha_3 d(d+\eta_2)\left(\frac{R_0}{R_1}-1\right)}$ and $R_0 < R_1 + \frac{\kappa\mu\alpha_1\beta_1\alpha_4\beta_4}{\alpha_3 d(d+\eta_1)(d+\eta_2)(d+\eta_4)(R_2-1)}$, the oncolytic M1 viruses in the absence of immune responses, partially succeed in lowering the concentration of tumor cells and increasing the normal cell's concentration. In this case, the treatment strategy is effective to remove the tumor cells to great extent but not completely. The simulations are shown in the Figures 5.1 and 5.2.

In Case VI, for $R_2 > 1, R_1 > \widetilde{R_q}$, $R_0 > R_1 + \frac{\kappa\mu\alpha_1\beta_1\alpha_4\beta_4}{\alpha_3 d(d+\eta_1)(d+\eta_2)(d+\eta_4)(R_2-1)}$, the simulations are given in the Figures 6.1 and 6.2. The efficacy of the treatment is reduced by the reduction in the concentration of the oncolytic viruses. The anti-tumour immune responses just prevent the tumour from getting worst but are unable to eradicate it completely.

The global stability of the equilibrium points indicates that the initial conditions do not affect the long run conduct of solutions. The simulated results are in excellent agreement with those given in [17]. The method successfully provides very accurate solutions in the different setting of parameters. The results are very accurate and obtained with less computational efforts.

10. Conclusion

The considered reaction-diffusion model for oncolytic cancer treatment virotherapy with immune responses is successfully solved by the implementation of the proposed cubic B-splines collocation method. It is also observed that the initial conditions do not affect in long run. The results achieved are quite satisfactory and competent with those available in [17]. The method being easy to implement, reliable and economical is appropriate for such reaction-diffusion models. Such an efficient approach for the numerical simulation of the reaction-diffusion model describing the dynamics of the oncolytic M1 virotherapy can be of great use for many biologists working on the cancer treatment leading strategies. Due to the complexity and the bigger dimensions of the virotherapy model the proposed cubic B-splines technique has advantages over the traditional numerical simulation techniques. The piecewise continuity and the differentiability of the cubic B-splines polynomials make the proposed technique best suitable for the numerical simulation of the considered reaction-diffusion model describing the dynamics of oncolytic virotherapy. For the future purposes, the application of the cubic B-splines collocation method is recommended as a burning alternative to deal a large class of similar models occurring in the field of medical sciences.

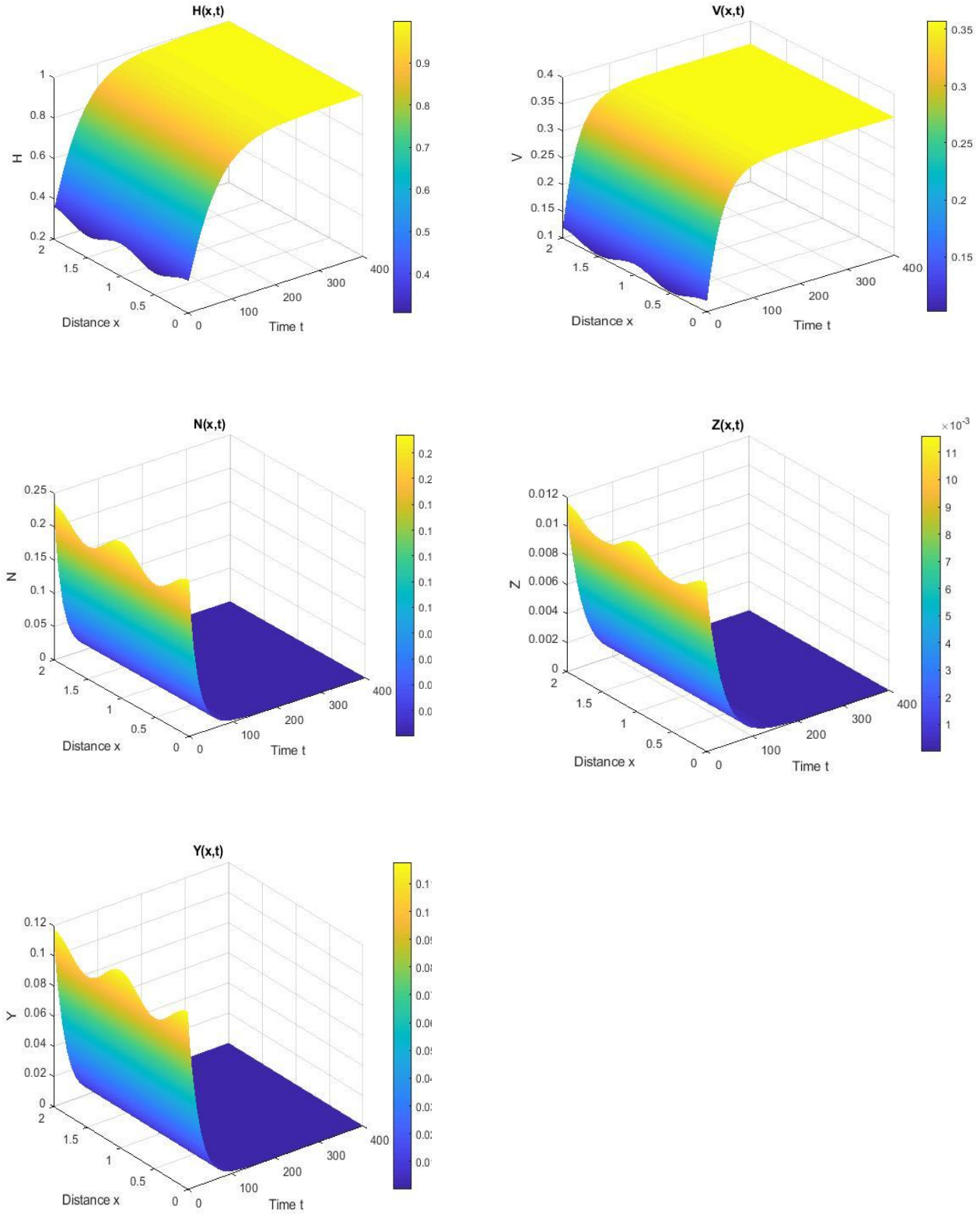

Figure 1: The numerical simulations for Case-I with cosine initial conditions.

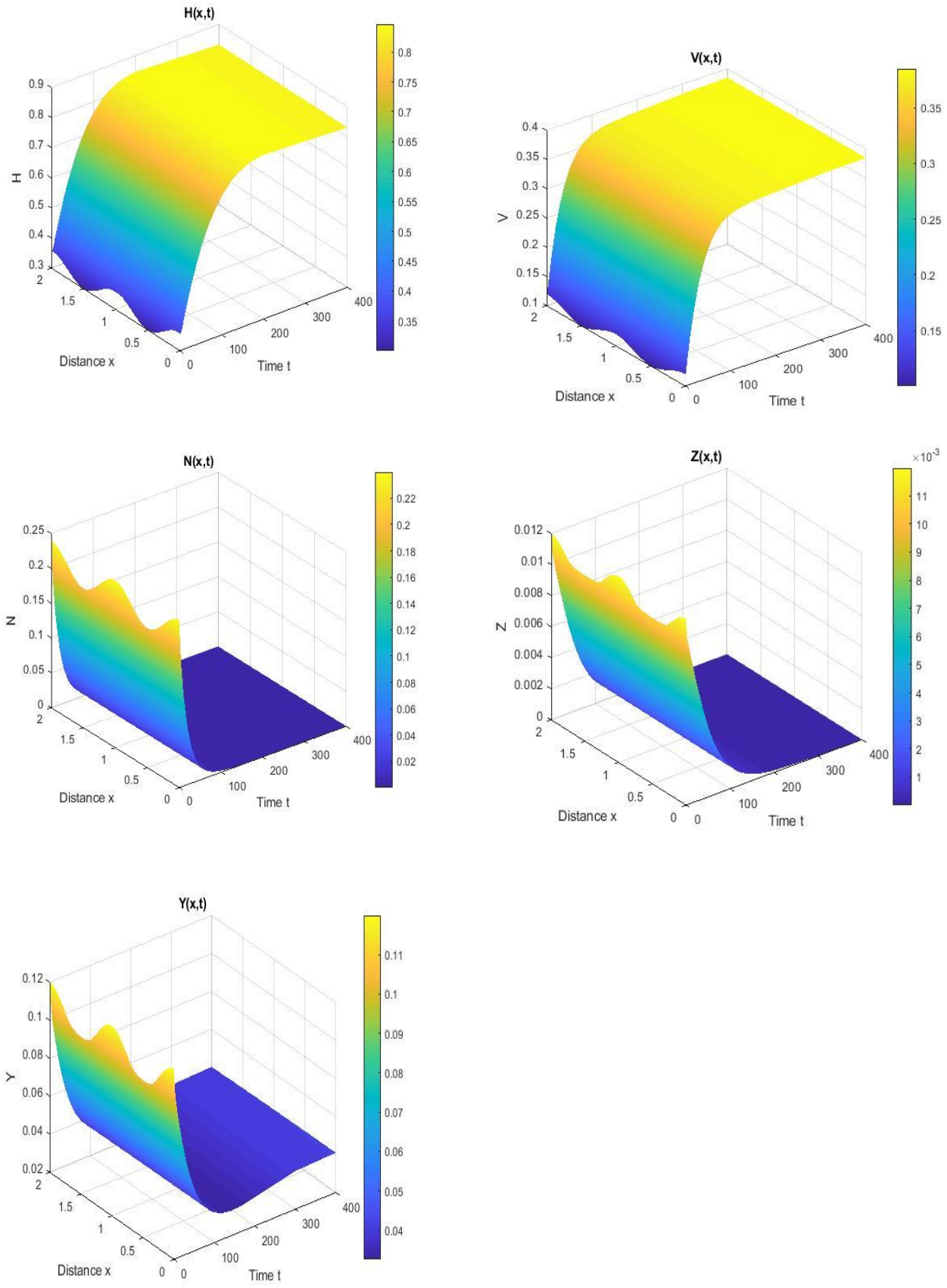

Figure 2: The numerical simulations for Case-II with cosine initial conditions.

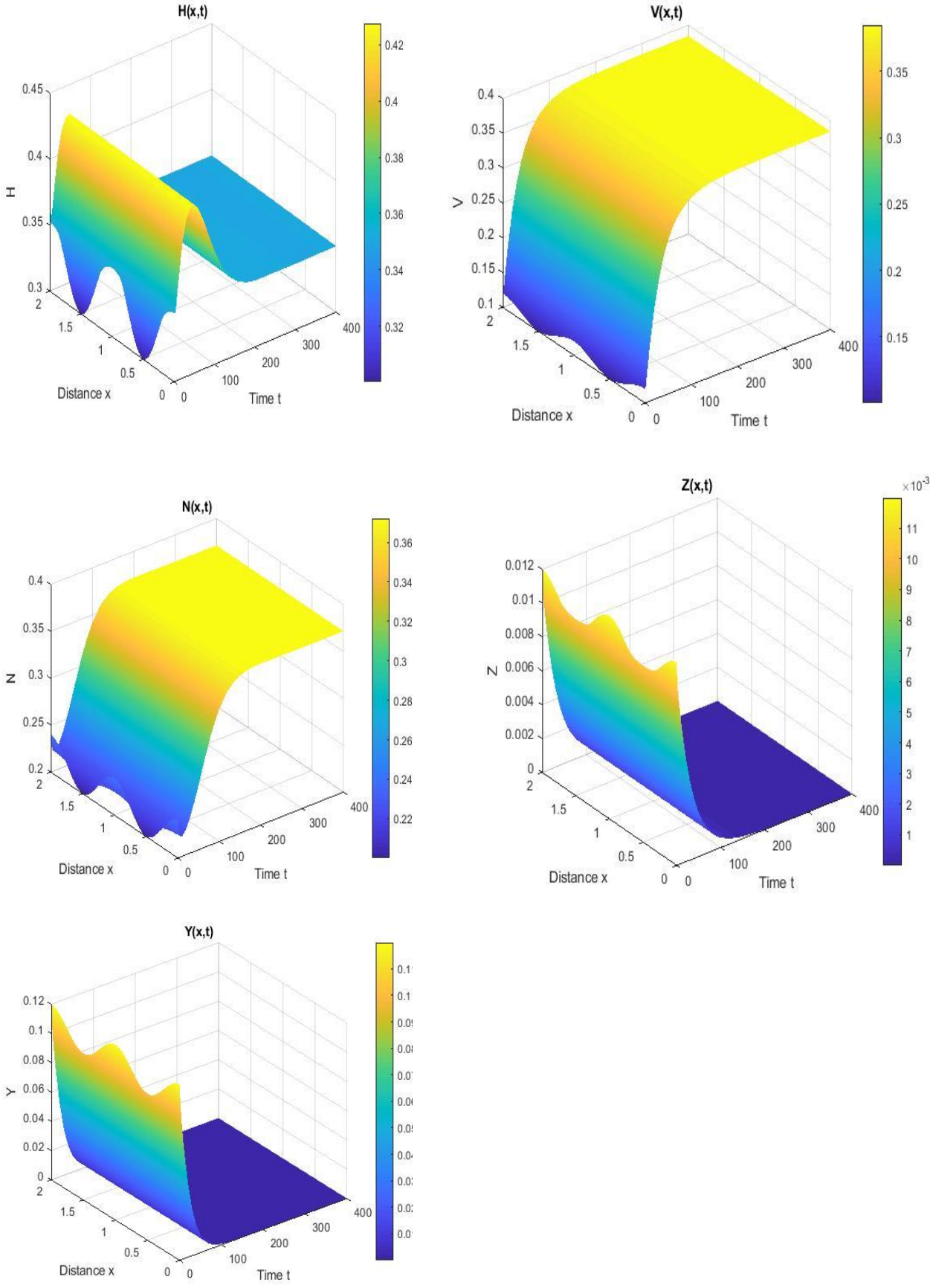

Figure 3: The numerical simulations for Case-III with cosine initial conditions.

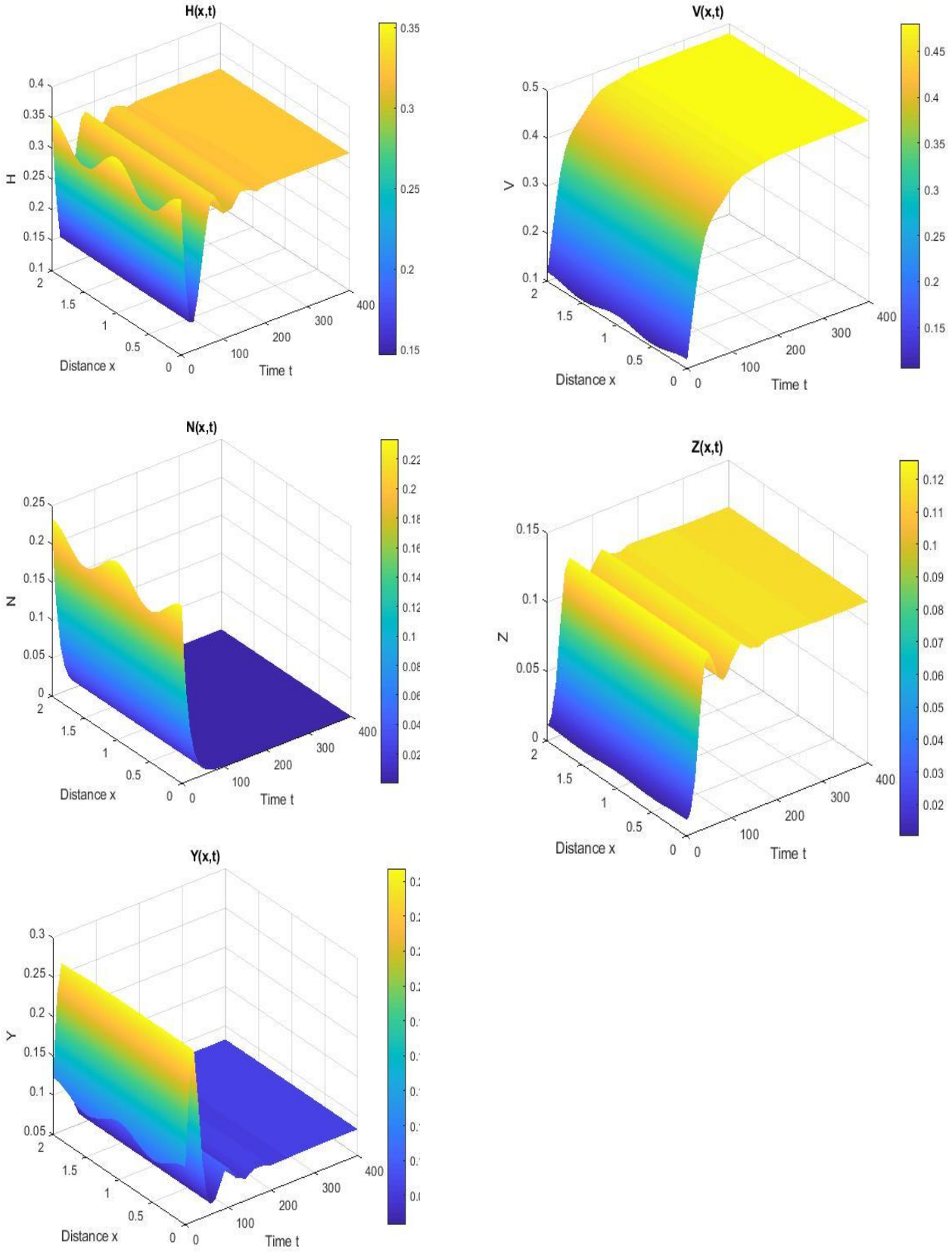

Figure 4: The numerical simulations for Case-IV with cosine initial conditions

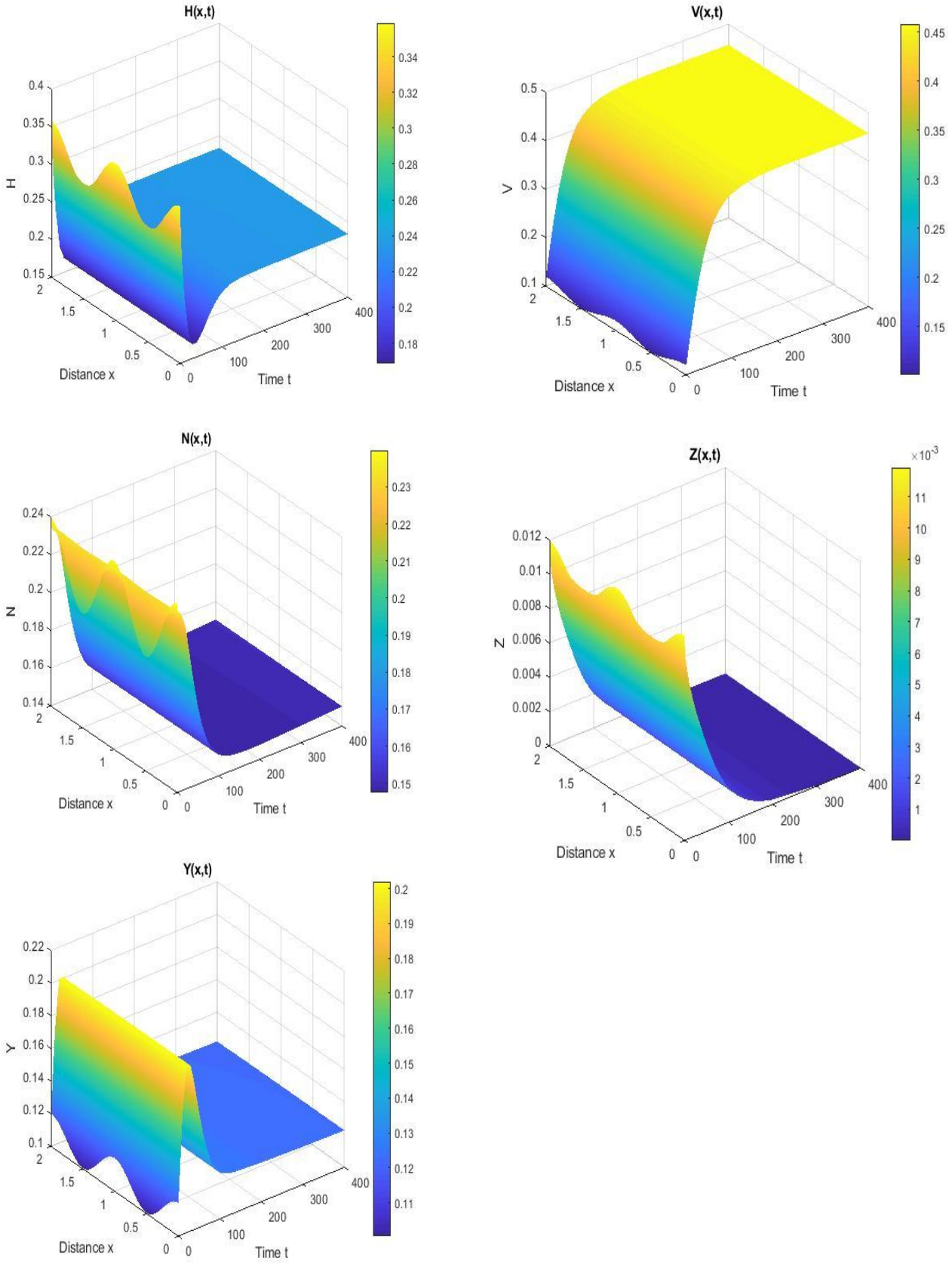

Figure 5: The numerical simulations for Case-V with cosine initial conditions.

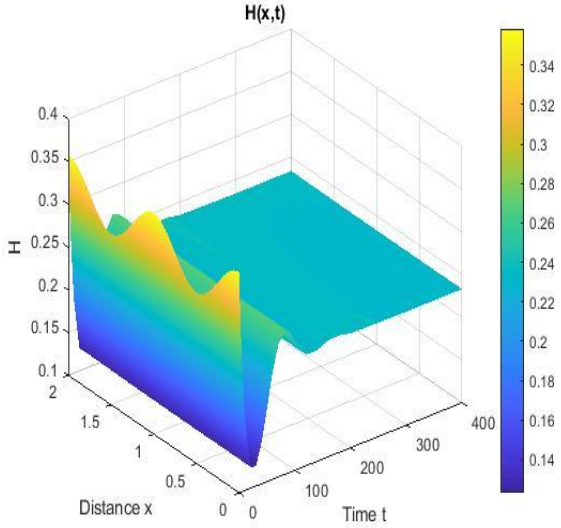
H(x,t)
H
Distance x
Time t

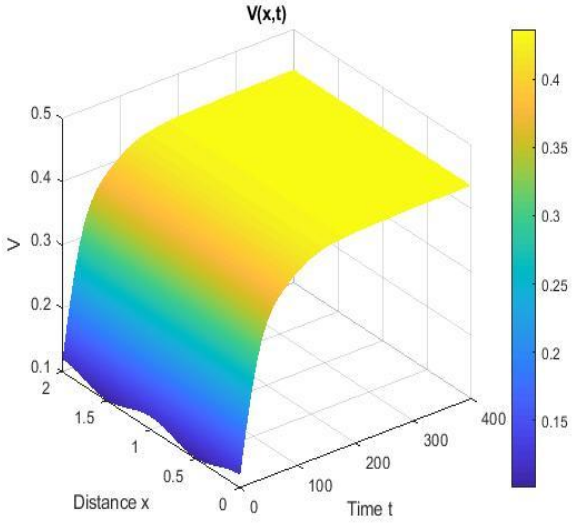
V(x,t)
V
Distance x
Time t

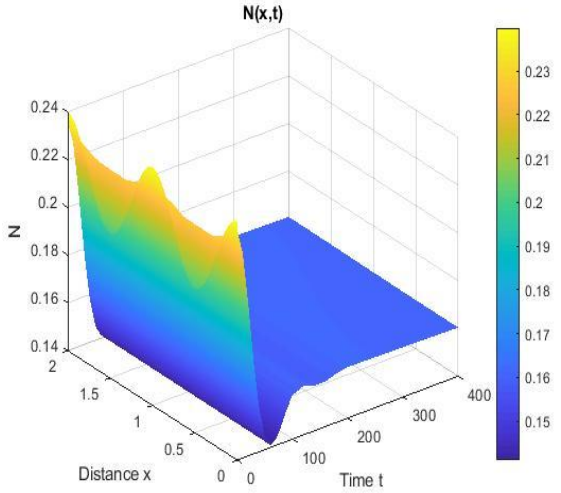
N(x,t)
N
Distance x
Time t

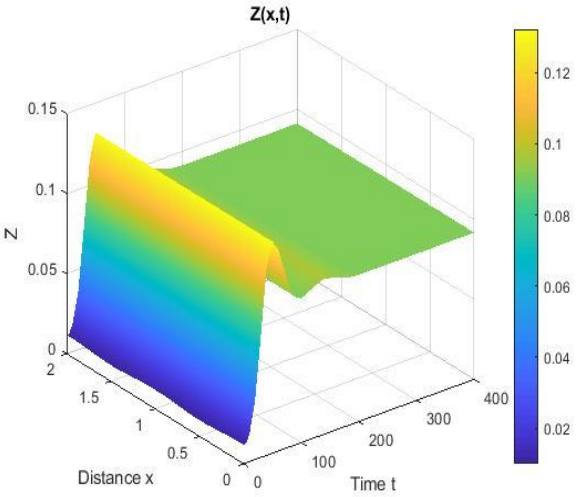
Z(x,t)
Z
Distance x
Time t

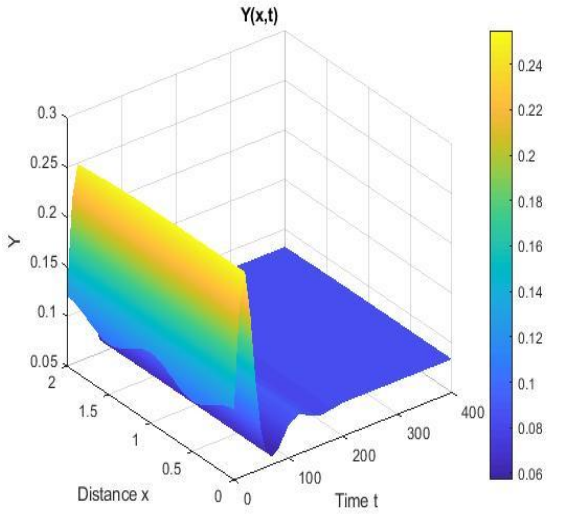
Y(x,t)
Y
Distance x
Time t

Figure 6: The numerical simulations for Case-VI with cosine initial conditions

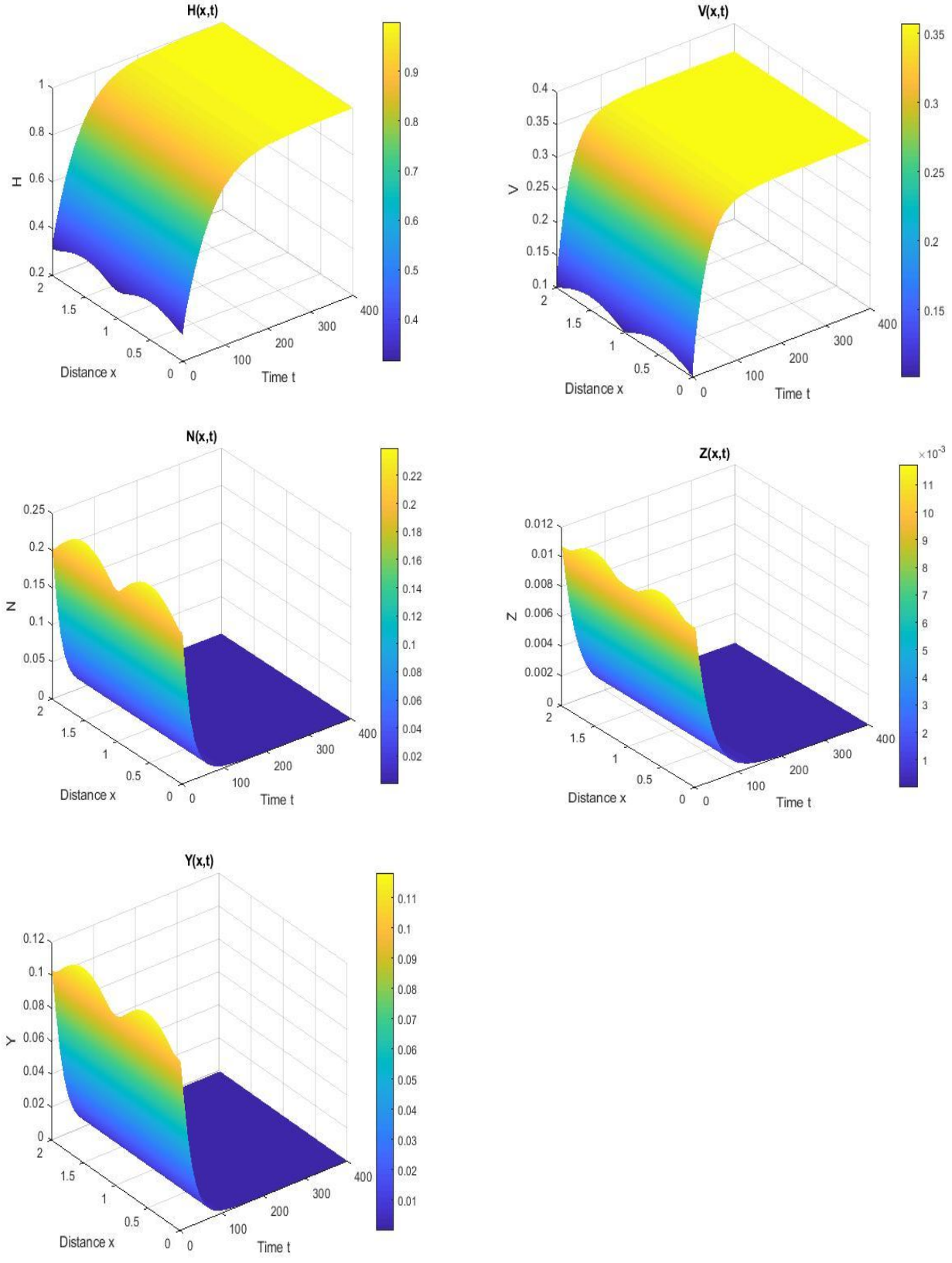

Figure 7: The numerical simulations for Case-I with sine initial conditions

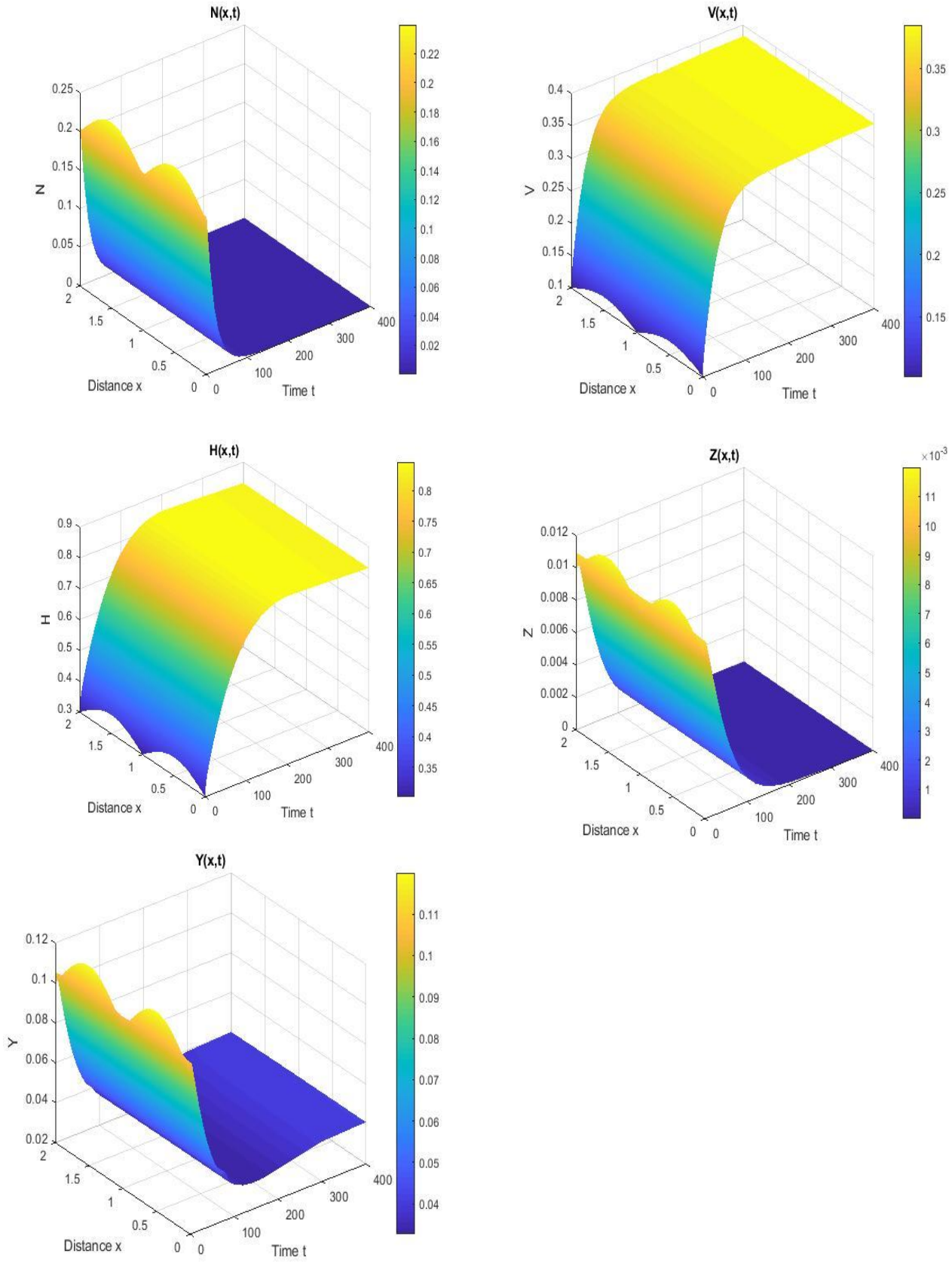

Figure 8: The numerical simulations for Case-II with sine initial conditions

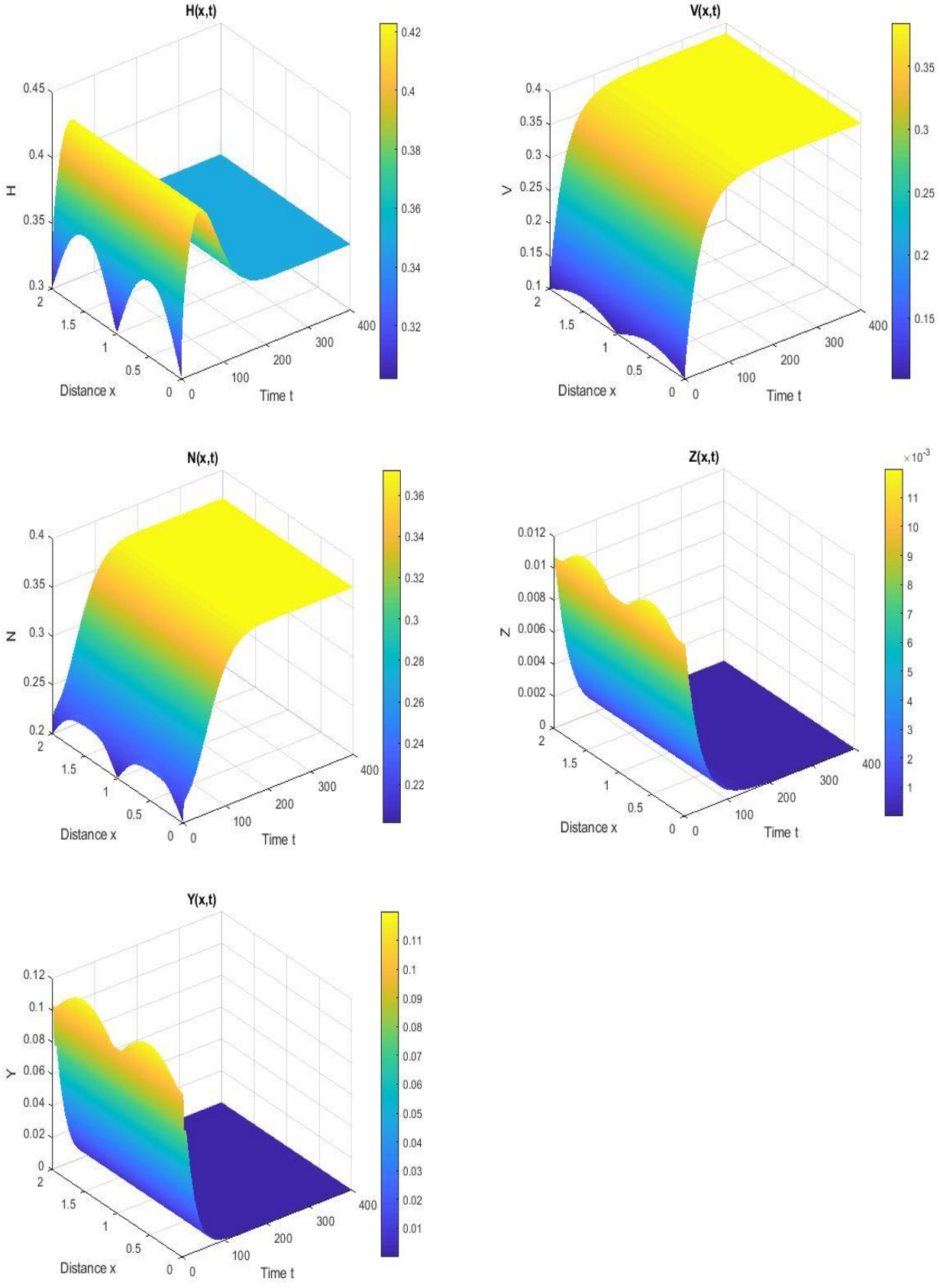

Figure 9: The numerical simulations for Case-III with sine initial conditions

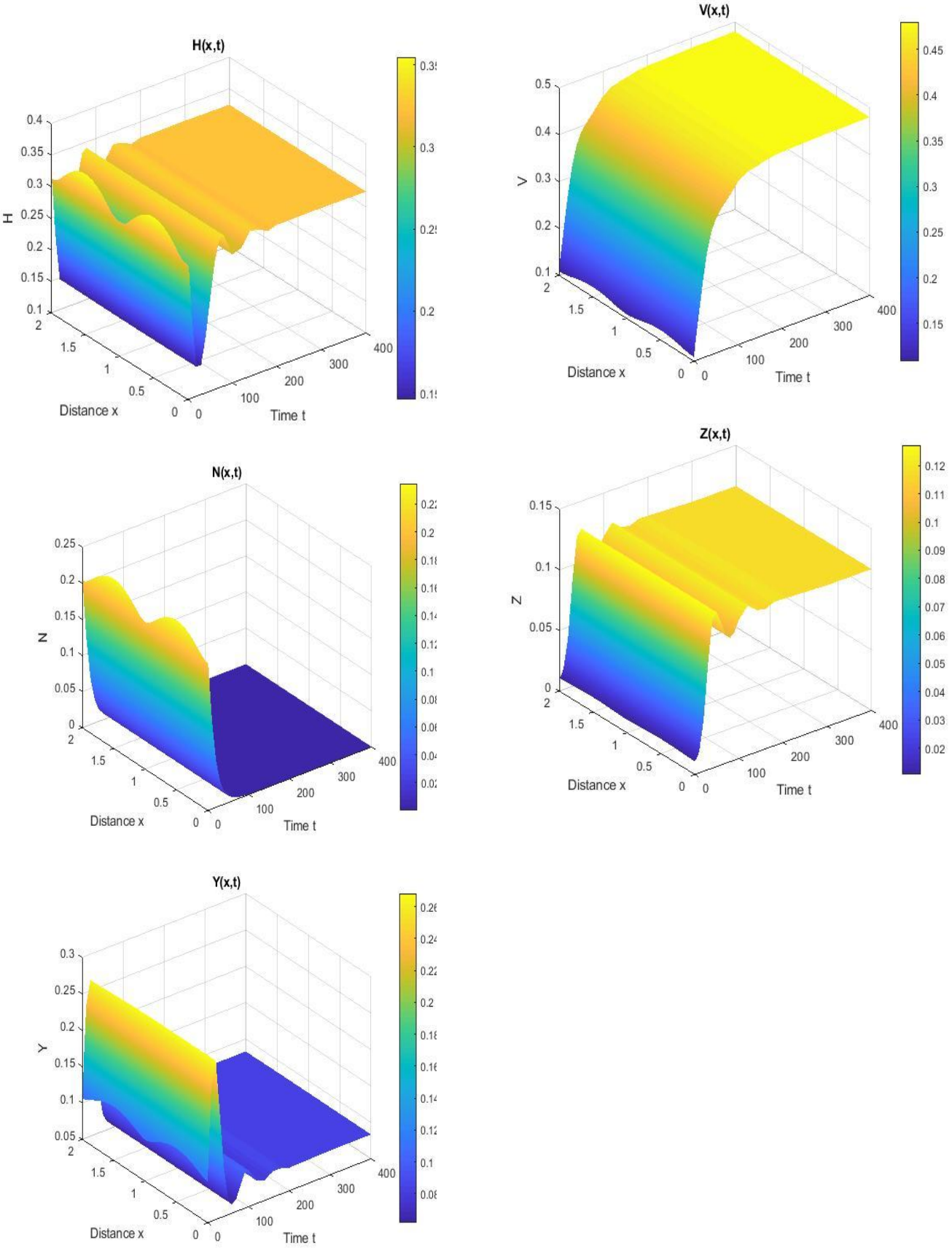

Figure 10: The numerical simulations for Case-IV with sine initial conditions

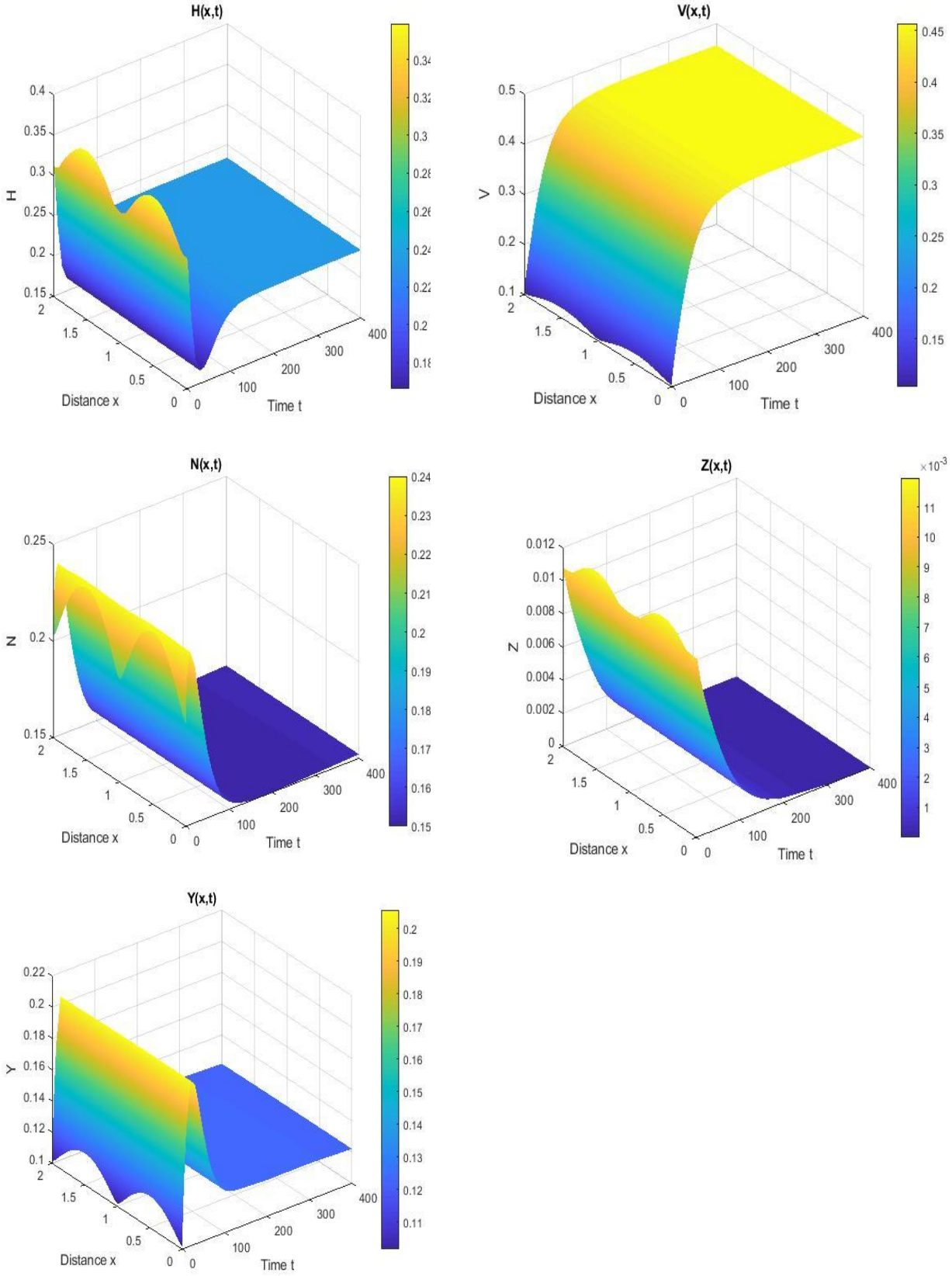

Figure 11: The numerical simulations for Case-V with sine initial conditions.

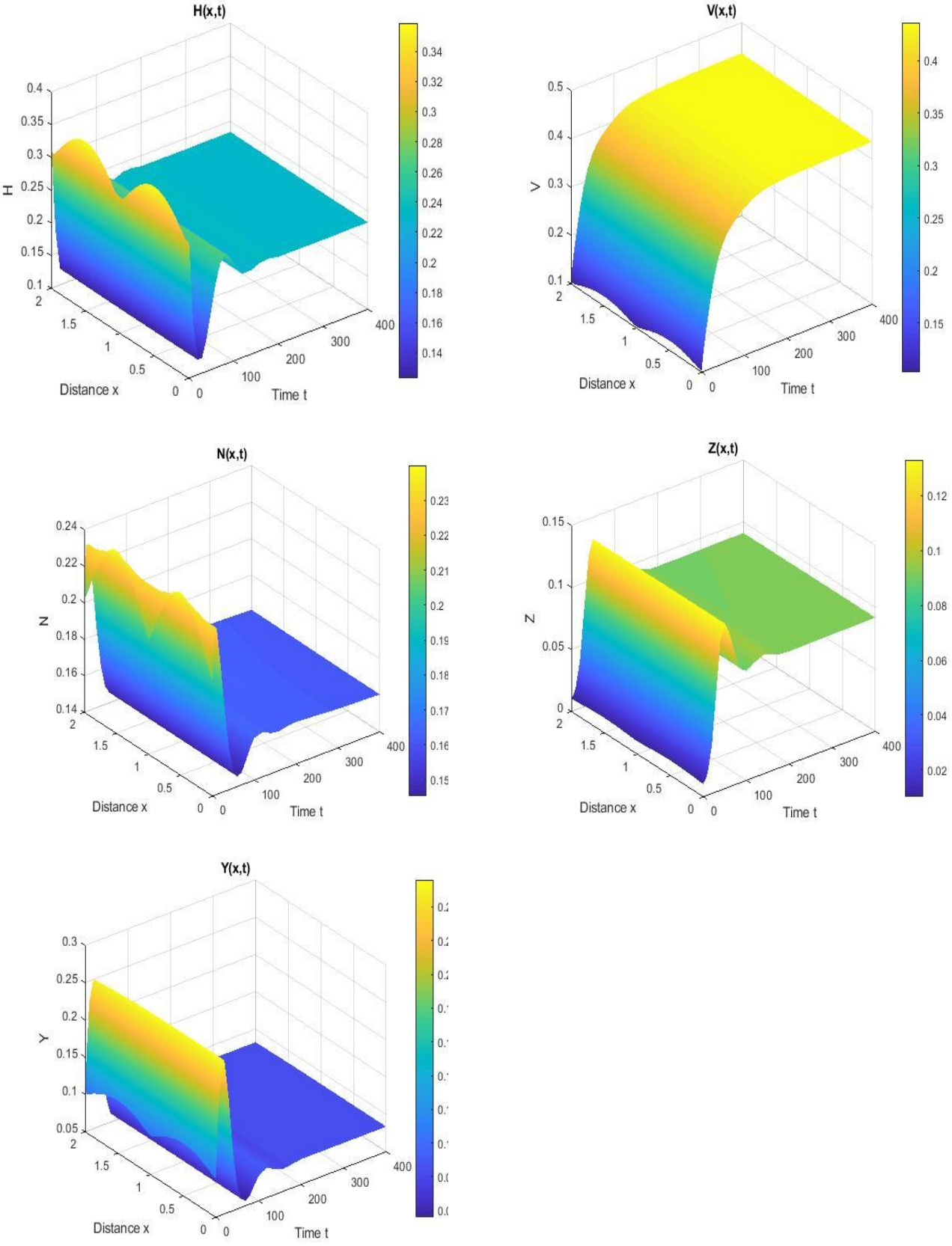

Figure 12: The numerical simulations for Case-VI with sine initial conditions

References

1. International Agency for Research on Cancer (IARC) (2020) World Health Organization (WHO), The GLOBOCAN 2020 database, Geneva.
2. Siegel R.; Miller K.; Fuchs H.; Cancer Statistics 2021, CA: A Cancer Journal for Clinicians, 2021, 71(1).
3. NIH: National Cancer Institute; Available at: https://www.cancer.gov/about-cancer/treatment/types
4. Wang Y.; Yang T.; He Q. (2020) Strategies for engineering advanced nanomedicines for gas therapy of cancer; National Science Review; 2020, 7, 1485-1512.
5. Gopisankar M. G.; Surendiran A. (2018) Oncolytic virotherapy – A novel strategy, Egyptian Journal of Medical Human Genetics (ELSEVIER), 19(3), 165-169.
6. Marelli G.; Howells A.; Lemoine N.R. (2018) Wang Y.; Oncolytic Viral Therapy and the Immune System: A Double-Edged Sword against Cancer; Front Immunol., 9, 11616-11623.
7. Malinzi J.; Sibanda P.; Mambili-Mamboundou H. (2015) Analysis of virotherapy in solid tumor invasion; Math Biosci. 263, 102-110.
8. Wang Y.; Tian J.; Wei. J. (2013) Lytic cycle: a defining process in oncolytic virotherapy, Appl. Math. Model. 37(8), 5962-5978.
9. Su Y.; Jia C.; Chen Y. (2016) Optimal control model of tumor treatment with oncolytic virus and MEK inhibitor, BioMed. Res. Int. 1-8.
10. Ratajczyk E.; Ledzewich U.; Schottler H. (2018) Optimal control for a mathematical model of glioma treatment with oncolytic therapy and TNF – $\boldsymbol{\alpha}$ inhibitors; J. Optim. Theort Appl. 176(2), 456-477.
11. Malinzi J.; Ouifki R.; Eladdadi A.; Torres K.A.J. White (2015) Enhancement of chemotherapy using oncolytic virotherapy: mathematical and optimal control analysis; Math. Biosci. Eng. 15(6), 1435-1463.
12. Wang Z.; Guo Z.; Peng H. (2017) Dynamical behavior of a new oncolytic virotherapy model based on gene variation; Discr. Contin. Dyn. Sys. Ser. S 10(5), 1079-1093.
13. Okamoto K.; Amarasekare P.; Petty I. (2014) Modeling oncolytic virotherapy: is complete tumor-tropism too much of a good thing? J. Theor. Biol. 358, 166-178.
14. Tao Y.; Guo Q. (2005) The competitive dynamics between tumor cells, a replication component virus and an immune response; J. Math. Biol. 51(1), 37-34.
15. Nowak, M.A.; May, R.M. (2000) Virus Dynamics: Mathematical Principles of Immunology and Virology; Oxford University: Oxford, UK.
16. Ren, X.; Tian, Y.; Liu, L.; Liu, X. (2018) A reaction-diffusion within-host HIV model with cell-to-cell transmission. J. Math. Biol. 76:1831–1872.
17. Elaiw, A.M.; Hobiny, A.D.; Al Agha, A.D. (2020) Global dynamics of reaction-diffusion oncolytic M1 virotherapy with immune response. Appl. Math. Comput. 367, 1–21.
18. Elaiw, A.M.; AlShamrani, N.H. (2018) Stability of an adaptive immunity pathogen dynamics model with latency and multiple delays. Math. Meth. Appl. Sci. 41, 6645–6672.
19. Miao, H.; Teng, Z.; Abdurahman, X.; Li, Z. (2017) Global stability of a diffusive and delayed virus infection model with general incidence function and adaptive immune response. Comput. Appl. Math. 37, 3780–3805.
20. Elaiw A.M.; Elnahary, E.K. (2019) Analysis of general humoral immunity HIV dynamics model with HAART and distributed delays. Mathematics 7, 157.
21. Elaiw, A.M.; Alshehaiween S.F.; Hobiny, A.D. (2019) Global properties of delay-distributed HIV dynamics model including impairment of B-cell functions. Mathematics 7, 837.
22. Elaiw, A.M.; Alshehaiween, S.F. (2020) Global stability of delay-distributed viral infection model with two modes of viral transmission and B-cell impairment. Math. Methods Appl. Sci. DOI:10.1002/mma.6408.
23. Elaiw, A.M.; AlShamrani, N.H. (2020) Stability of a general adaptive immunity virus dynamics model with multi-stages of infected cells and two routes of infection. Math. Methods Appl. Sci. 43, 1145–1175.
24. Anderson, R.; May, R.; Gupta, S. (1989) Non-linear phenomena in host-parasite interactions. Parasitolog 99, S59–S79.
25. Anderson, R. (1998) Complex dynamic behaviours in the interaction between parasite populations and the host's immune system. Int. J. Parasitol 28, 551–566.
26. Saul, A. (1998) Models for the in-host dynamics of malaria revisited: errors in some basic models lead to large over-estimates of growth rates. Parasitology 117, 405–407.
27. Gravenor, M.; Lloyd, A. (1998) Reply to: Models for the in-host dynamics of malaria revisited: errors in some basic models lead to large over-estimates of growth rates. Parasitology 171, 409–410.
28. Iggidr, A.; Kamgang, J.; Sallet, G.; Tewa, J. (2006) Global analysis of new malaria intrahost models with a competitive exclusion principle. SIAM J. Appl. Math. 67, 260–278.

29. Saralamba, S.; Pan-Ngum, W.; Maude, R.; Lee,;Tarning, J.; Lindegårdh, N.; Chotivanich, K.; Nosten, F.; Day, N. ; Socheat, D.; White, N.; Dondorp, A.; White, L. (2011)Intrahost modeling of artemisinin resistance in Plasmodium falciparum. Proc. Natl. Acad. Sci. 108, 397–402.
30. Demasse, R.; Ducrot, A. (2013) An age-structured within-host model for multistrain malaria infections. SIAM J. Appl. Math. 73, 572–593.
31. Song, T.; Wang, C.; Tian, B. (2019) Mathematical models for within-host competition of malaria parasites. Math. Biosci. Eng. 16, 6623–6653.
32. Elaiw, A.M.; Agha, A.D. Al. (2020) Global Analysis of a reaction-diffusion within-host malaria infection model with adaptive immune responses, MDPI, Mathematics 8, 563.
33. Mittal, R.C.; Jain, R.K. (2012) Cubic B-splines collocation method for solving nonlinear parabolic partial differential equations with Neumann boundary conditions, Commun Nonlinear Sci NumerSimulat, 17, 4616-4625.
34. Mittal, R.C.; Tripathi, A. (2014) A collocation method for numerical solutions of Coupled Burger's equations, International Journal for computational methods in engineering science and mechanics, 15: 457-471.
35. Mittal, R.C.; Jain, R.K.; (2012) Numerical solutions of nonlinear Burger's equation with modified cubic B-splines collocation method, Appl. Math. Comput.
36. Mittal, R.C.; Jain, R.K. (2012) Redefined cubic B-splines collocation method foe solving convection-diffusion equations, Applied Mathematical Modeling, 36,5555-5573.
37. Mittal, R.C.; Jain, R.K. (2012) Numerical solutions of non-linear Burger's equation with modified cubic B-splines collocation method, Applied Mathematics and Computation (Elsevier) 218, Issue 15, 7839-7855.
38. Mittal, R.C.; Arora, G. (2010) Efficient Numerical Solution of Fisher's equation by using B-spline method, International Journal of Computer Mathematics (Taylor & Francis) 87, No. 13, October 2010, 3039-3051.
39. Rohilla, R.; Mittal, R.C. (2018) Numerical study of reaction diffusion Fisher's equation by fourth order cubic B-splines collocation method, Mathematical Sciences, Cross Mark (Elsevier), 12, 79-89.
40. Hetzel, C.; Anderson, R. (1996) The within-host cellular dynamics of blood stage malaria, Theoretical and experimental studies. Parasitology, 113, 25–38.
41. Tumwiine, J.; Mugisha, J.; Luboobi, L. (2008) On the global stability of the intra-host dynamics of malaria and the immune system. J. Math. Anal. Appl. 341, 855-869.
42. Cont, S.D.; Boor, C.; Elementary Numerical Analysis: An Algorithmic Approach, McGraw-Hill Book Company.
43. Martin, A.; Boyd, I. (2010) Variant of the Thomas Algorithm for opposite-bordered tri-diagonal systems of equations, Int. J. Num. Meth. Biomedical Engg. 26(6), 752-759.
44. Unser, M. (2002) Splines: A Perfect fit for medical imaging, Proceedings of SPIE, Int. Soc. Optical Engg.4684
45. Hale J.K.; Lunel S.M.V. (1993) Introduction to Functional Differential Equations, Springer-Verlag, New York.
46. Henry D. (1993) Geometric Theory of Semilinear Parabolic Equations, Springer-Verlag, New York.
47. Wang L.; Li M. (2001) Diffusion driven instability in reaction-diffusion systems; J. Math. Anal. Appl. 254(1), 138-153.
48. Wang Z.; Guo Z.; Peng H. (2016) A Mathematical model verifying potent oncolytic efficacy of M1 virus, Math. Biosci. 276, 19-27.
49. Mittal R.C.; Goel R.; Ahlawat N. (2021) An Efficient numerical simulation of a reaction-diffusion malaria infection model using B-splines collocation, Chaos, Solitons, Fractals143, 110566.